

LAPPEENRANTA UNIVERSITY OF TECHNOLOGY

Faculty of Technology

Department of Electrical Engineering

Master's Thesis

**Jari Honkanen**

**ROBUST CURRENT CONTROL OF A PHASE SHIFTED  
FULL-BRIDGE BUCK CONVERTER**

Examiners: Prof. Pertti Silventoinen

D.Sc. Juha-Pekka Ström

Instructor: M.Sc. Jussi Karttunen

Lappeenranta August 14, 2014

# ABSTRACT

Lappeenranta University of Technology  
Faculty of Technology  
Department of Electrical Engineering

Jari Honkanen

## **Robust current control of a phase shifted full bridge buck converter**

Master's thesis

2014

47 pages, 12 figures and 1 table.

Examiners: Prof. Pertti Silventoinen

D.Sc. Juha-Pekka Ström

Keywords: Switch mode power supply, digital control, robust control

In this thesis, the main point of interest is the robust control of a DC/DC converter. The use of reactive components in the power conversion gives rise to dynamical effects in DC/DC converters and the dynamical effects of the converter mandates the use of active control. Active control uses measurements from the converter to correct errors present in the converter's output. The controller needs to be able to perform in the presence of varying component values and different kinds of disturbances in loading and noises in measurements. Such a feature in control design is referred as robustness. This thesis also contains survey of general properties of DC/DC converters and their effects on control design. In this thesis, a linear robust control design method is studied. A robust controller is then designed and applied to the current control of a phase shifted full bridge converter. The experimental results are shown to match simulations.

# TIIVISTELMÄ

Lappeenrannan teknillinen Yliopisto

Teknillinen tiedekunta

Sähkötekniikan koulutusohjelma

Jari Honkanen

**Robusti virta säätö vaihesiirretyissä kokosilta buck muuntimessa**

Diplomityö

2014

47 sivua, 12 kuvaa ja 1 taulukko.

Tarkastajat: Prof. Pertti Silventoinen

TkT Juha-Pekka Ström

Avainsanat: Hakkuri, digitaalinen säätö, robusti säätö

Tämän työn pääkohta on robustin säädön käyttö DC/DC muuntimessa. Reaktiivisten komponenttien käyttäminen tehon muokkauksessa usein tekee aktiivisen säädön välttämättömäksi. Aktiivinen säätö käyttää mittauksia laitteesta korjaamaan virheitä laitteen lähtösignaalissa. Säädön on toimittava ilman, että komponenttien arvojen vaihtelu, kuormituksen muutokset tai mittauskohina vaikuttavat toimintaan. Tämänlaista toimintaa nimitetään robustisuudeksi. Työssä esitellään myös muuntimien yleisiä ominaisuuksia, jotka vaikuttavat säädön suunnitteluun. Tässä työssä esitään lineaarinen robustin säädön suunnittelumenetelmä ja sitä käytettiin muuttajan säädön suunnitteluun. Suunniteltu säätö testattiin laboratoriossa ja mitatun askelvasteen todettiin olevan lähellä mallinnettua vastetta.

## Acknowledgements

This thesis was written in Lappeenranta during the spring and summer of 2014. The work documented in this thesis was part of a research project concerning digital control and its benefits that was done in collaboration with Powernet.

I want to thank the powernet guys, especially Samuli, for your collaboration.

I want to thank professor Pertti Silventoinen for his patience and encouragement.

Special thanks to Juha-Pekka Ström and Janne Hannonen with whom I've had the privilege to be work with for the past 2 years during the project.

I also want to thank Jussi Karttunen for his help with this thesis.

Jari Honkanen

August 2014

Lappeenranta, Finland

# Contents

<b>1</b>	<b>Introduction</b>	<b>4</b>
1.1	Control of dynamical systems . . . . .	5
1.2	Goal of this thesis . . . . .	8
1.3	Thesis outline . . . . .	9
<b>2</b>	<b>Survey of robust control methods</b>	<b>10</b>
2.1	Briefly on robust control methods . . . . .	10
2.1.1	Linear quadratic gaussian control . . . . .	11
2.1.2	Nonlinear robust control based on Lyapunov function . . . . .	11
2.1.3	Sliding mode control . . . . .	13
2.1.4	Internal Model Control and disturbance rejection control . . . . .	13
2.1.5	$\mathcal{H}_\infty$ control . . . . .	14
2.2	Robust control design methods . . . . .	14
<b>3</b>	<b>Control Design Considerations</b>	<b>17</b>
3.1	Classical robust design . . . . .	17
3.1.1	Control construction based on sensitivity analysis . . . . .	20
<b>4</b>	<b>Overview of loop shaping <math>\mathcal{H}_\infty</math> control design</b>	<b>22</b>
4.1	Stabilizing $\mathcal{H}_\infty$ control . . . . .	23
4.1.1	State-Feedback form of stabilizing $\mathcal{H}_\infty$ controller . . . . .	24
4.2	Loop Shaping $\mathcal{H}_\infty$ controller . . . . .	25
<b>5</b>	<b>Switch-mode power supply control</b>	<b>27</b>
5.1	Limitations of switching converter control . . . . .	27
5.1.1	Switching frequency . . . . .	28
5.1.2	Digital calculation cycle . . . . .	28
5.1.3	Limitation by bounded states . . . . .	28
5.1.4	Unstable zero dynamic . . . . .	29

5.2	Robust control of phase shifted full-bridge buck converter . . . . .	29
5.2.1	Dynamic behavior . . . . .	32
5.2.2	Control objectives . . . . .	33
5.2.3	Robust control design for current loop . . . . .	34
5.3	Digital control implementation . . . . .	36
5.3.1	Control code structure . . . . .	37
5.3.2	Test measurements . . . . .	39
<b>6</b>	<b>Notes and discussion</b>	<b>42</b>
	<b>References</b>	<b>47</b>

# CONVENTION AND NOTATION

## SUBSCRIPTS

U, v	voltage
out	output, for example $U_{out}$ refers to output voltage
I, i	current
in	input

## ACRONYMS

AD	Analog to Digital (converter)
d	Duty ratio
DA	Digital to Analog (converter)
DC	Direct Current
ESR	Equivalent series resistance
ESL	Equivalent series inductance
PID	Proportional-Integral-Derivative controller
PFC	Power Factor Correction
PWM	Pulse Width Modulation

# 1 Introduction

Devices that are powered with electric energy are compiled of many different sub-circuits that perform different parts of the whole operation. Different parts inside an electronic device require many different voltage levels. The voltages might vary only by a few volts to several kilo volts, for example in a medium voltage converter which is controlled by a 3.3 V microprocessor. It is typical that all of the different voltage levels are made from the same power line and that a commercial system needs to work with different mains voltages. The mains ac line-to-line voltage varies from 90 VAC to 240 VAC globally which translates to wide range of possible input voltages. The wide variation of used voltage requires some form of voltage level translation.

It was standard method for the different voltage levels inside an electrical system to be supplied with a mains frequency transformer. The transformer circuit does not provide the properly regulated voltage levels and thus a regulator is required. The different mains voltage levels were taken into account by using separate windings in the transformer. The power supplies had linear regulators that stabilized the voltages to proper levels. The linear supply works so that the excess voltage is dissipated in regulators acting as resistive elements. All of the load current is passed through the resistive element, which results in a power loss. This power loss is the power that is wasted as heat and therefore lowers the overall efficiency of the power supply (Erickson and Maksimovic, 2001).

Modern power supplies are commonly constructed with transistors acting as switches. The switching action lends its name to the switched mode power supply. The switches work in frequencies from few kilohertz to lower megahertz range, which reduces the size of magnetic components and capacitors compared to mains frequency components. The power is translated between voltage levels with reactive components. The switch mode power supply therefore ideally has unity efficiency as resistive elements

are not used for the power conversion. The efficiency in real circuit can never be 100 %, but with proper design a 90 % and above efficiencies are achievable. High efficiency also relaxes the requirement for heat transfer, which reduces the circuit size. In some cases, such as portable battery operated equipment, high efficiency is very important as it reduces the power consumption and increases the battery life. Due to the benefits of switched mode power converters, they are very commonly used in power supplies.

## **1.1 Control of dynamical systems**

The usage of reactive components in a switch mode power supply makes the system dynamical. Inductance stores energy in the magnetic field and capacitances store energy as electric charge. The stored energy can oscillate between the inductances and capacitances. Because of the inherent oscillating properties, the switch mode system usually needs active control in order for the power supply to function properly. Active control refers to a method where the input signal that feeds the system is modified based on measurements taken from output signal. The control is commonly designed using a mathematical model for the dynamics of the controlled system, which is commonly referred in the control context as plant. The overall control design is an iterative process with possibly multiple stages of modeling and model verification, control design, and simulations and lastly test measurements (Skogestad and Postlethwaite, 2007).

The control system model is usually formulated as a set of differential equations. The set of differential equations is called a state-space and the system's variables are states. In the state-space model, the system's state-variables represent a coordinate system and the evolution of the states can be thought as motion in the state-space (Goodwin et al., 2001). This allows for extensive mathematical analysis of the system with differential algebraic and geometric methods.

The choice of variables is not unique and the designer has a lot of flexibility in choosing

the proper coordinate system. Although the coordinates are not unique, the choice of coordinate system is not arbitrary. The resulting system needs to be controllable or at least reachable, which means that the system needs to be formulated so that the whole state is determined by the chosen state variables and that the chosen output variables can be influenced by the applied input (Goodwin et al., 2001) (Åström and Wittenmark, 2011).

The change between coordinate systems can be accomplished by coordinate transforms, that map the measured variables of the system desired to the state-space. Very common use of state transformations is in digital filter and control implementation, where different structures of the digital system are defined by different choice of coordinate axes. Typical implementations are direct form I and II and their different cascade structures. Cascade structures are used to construct higher order systems by cascade connection of usually first and second order systems. Different structures are used to minimize noise and loss of accuracy that stems from finite word length of the digital processor (Taylor and Mellott, 1998). With ideal infinite word lengths, all different structures would have exactly the same input-output characteristics. (Taylor and Mellott, 1998)

It is also convenient, if possible, to define the states to be same as the measurements as this makes the signals inside the controller to have some physical meaning. For example, the LCR circuit in Figure 1.1 the states can be chosen as the voltage of the capacitor and current of the inductor. This choice of variables yields the state-equation given in (1.1)-(1.2). Alternatively, the variables can be chosen as the capacitor voltage and its first derivative, which yields the state equation (1.3)-(1.4). Both state-space representations define the same input-output mapping from input voltage to capacitor voltage. The difference in this case comes from the choice of the second state which is either inductor current or a derivative of the capacitor voltage. The choice of variables effect the control design as in the controller construction the states are fed back to the input to produce the control action.

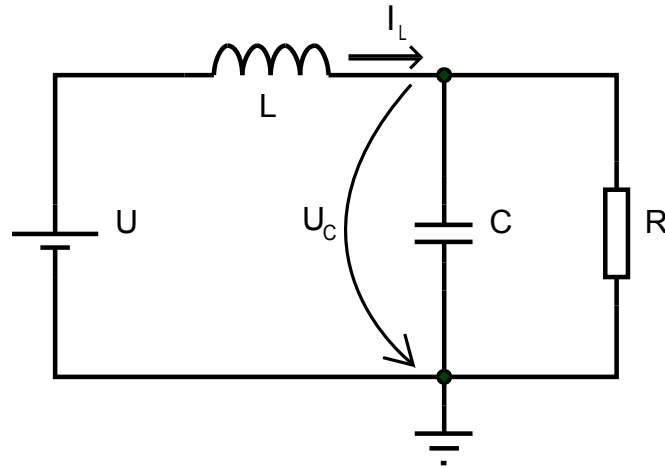


Figure 1.1. Schematic of LCR circuit with current and capacitor voltage shown as possible choice of measurements.

$$\dot{i}_L = -\frac{u_C}{L} + \frac{u_{in}}{L} \quad (1.1)$$

$$\dot{u}_C = \frac{i_L}{C} - \frac{u_C}{RC} \quad (1.2)$$

$$\dot{x}_1 = x_2 \quad (1.3)$$

$$\dot{x}_2 = -\frac{x_1}{RLC} - \frac{x_2}{RC} + \frac{u_{in}}{RLC} \quad (1.4)$$

$$x = [u_C, \dot{u}_C]^T$$

Along with state-space models, systems can be defined with transfer functions. Transfer functions model the system's input signals to some outputs. The transfer function method allows for analysis in the frequency plane, where system's gain is referenced against a frequency. Transfer functions are commonly used not only for the analysis of controlled inputs to system outputs, but also for modeling system's disturbances and noise effects on the inputs and outputs. Usually in control system design, the most important transfer functions are those that model the effects of system's controlled input voltage to the controlled output and noise effects from to input and output. (Skogestad and Postlethwaite, 2007)

Both, transfer function and state-space, are used to model and analyze different properties of the system. Stability can be defined from either the state-space or from the transfer functions. Frequency response is only attained from the transfer functions. The transfer functions can only be defined for linear, time invariant systems (Goodwin et al., 2001). Many switch mode topologies are inherently nonlinear, or made nonlinear with for example nonlinear current control (Smedley, 1991). In these cases, it is common to use linearization techniques to obtain a linear model from which the system's frequency properties can be attained (Erickson and Maksimovic, 2001). The controller itself can also be designed and analyzed in the frequency domain.

State-equations provide a framework where time domain properties of a system can be described. State-space is also useable in case of nonlinear and non-smooth state equations (Freeman and Kokotović, 1996). Nonlinear system's stability can be defined with a Lyapunov function which guarantees the stability of the system everywhere where the Lyapunov derivative is negative (Haddad and Chellaboina, 2008). The controller can be designed using the state-space equations in both linear and nonlinear cases using methods based on Lyapunov functions (Haddad and Chellaboina, 2008).

Regardless of the method used for control design, the goal of feedback design is to provide a controlled system which will perform under varying component values and uncertainty in the measurements and used modeling method. The property of control being able to handle discrepancies between the modeled and a real system is called robustness.

## **1.2 Goal of this thesis**

Robustness in control systems means that the controlled system can operate satisfactorily under inevitable errors in the actual system and the simulated model. This thesis aims to clarify why robustness should be chosen as design factor when a control for

DC/DC converter is designed.

### **1.3 Thesis outline**

The main subject of this thesis is the  $\mathcal{H}_\infty$  control of a full bridge buck DC/DC converter. In second chapter, the reasoning behind choosing  $\mathcal{H}_\infty$  control over other robust methods is explained in addition to the design considerations. Sensitivity analysis is outlined and used to analyze the designed controller. The chosen  $\mathcal{H}_\infty$  control method is used to design controller for phase shifted DC/DC buck converter. The controller is implemented in digital domain and programmed into a microprocessor. Considerations on implementing digital control are described shortly. Robust control system design and implementation with laboratory measurements are presented in chapter 5. Lastly, chapter 6 contains discussion on the benefits and constraints of the used control method.

## **2 Survey of robust control methods**

Uncertainty comes from a mismatch between the signals in a modeled system and the actual system. Uncertainty means that the model does not predict accurately the system's internal states or outputs even if the input is perfectly known. The inherent errors of all mathematical models comes from unmodeled dynamics and disturbances in either the states or measurements and errors in the model's parameters. The errors are always present to at least to some extent, since no real system is neither linear, of finite order. The unavoidable discrepancies are commonly mitigated by the use of control. When the uncertainty is analyzed and its effects are accounted for during the control design, the resulting control system is commonly referred as being robust (Skogestad and Postlethwaite, 2007).

### **2.1 Briefly on robust control methods**

Control law which is designed with robustness as a design factor is commonly referred as robust control. The robustness in a robust control is a measurable entity which states some mathematically defined boundaries within which the system can be guaranteed to operate. Commonly the used mathematical framework for robust design is normed function spaces, which lends itself to bounds for the states and inputs that are defined with proper norms (Haddad and Chellaboina, 2008). Norm can be thought of a specific measure of the size of a mathematical object.

There are many different control methods that are regarded as robust control in both nonlinear and linear control theory. The following list is not exhaustive and there exists theories beside those outlined in this thesis. Control methods that are considered robust are for example model predictive control (Brosilow and Joseph, 2002), internal model control (Brosilow and Joseph, 2002), sliding mode control (Utkin, 1977) and adaptive

control (Krstic et al., 1995).

### **2.1.1 Linear quadratic gaussian control**

The LQG control is a special case of optimal control design that minimizes the  $\mathcal{H}_2$  norm, due to use of Kalman filter as the state observer. Kalman filter is the best linear filtering method for signals that have known constant statistical properties in a sense that it minimizes the root-mean squared error of the estimate (Simon, 2006). The LQG control differs from all control methods mentioned in the following section in that there are no guaranteed robustness margins to be defined by the design method despite its ability to very effectively block random noises in measurements. The counterexample of a robust design of LQG control was shown in (Doyle, 1978). Robustness of a LQG controller can be recovered by using loop transfer recovery methods (Doyle and Stein, 1981) and by introducing artificial noise in the frequencies where uncertainties reduce the robustness (Moore et al., 1981).

### **2.1.2 Nonlinear robust control based on Lyapunov function**

The Lyapunov function is a positive definite function whose derivative is negative definitive. The existence of a Lyapunov function is sufficient to prove stability of a dynamical system (Lyapunov, 1892). The Lyapunov theory in nonlinear control is used to design a control law alongside with a Lyapunov function that guarantees stability. The Lyapunov function based control method also allows for beneficial dynamics (linear or nonlinear) to be exploited in the control design as the control law is directly derived from the system's dynamics (Haddad and Chellaboina, 2008).

Optimality of control is defined using a cost function which is defined by a Hamiltonian-Jacobi-Bellman (HJB) equation (Sontag, 1998). The robustness can be designed into

the control by means of proper formulation of the cost functional (Sepulchre et al., 1997). Due to difficulties in solving the HJB function associated with the cost functional, the solution is obtained in inverse fashion by proving that a certain type of controller is a solution to some cost functional (Freeman and Kokotović, 1996; Sontag, 1998). The achieved robustness margins are defined by the controlled system's nonlinear gain and disc margins (Sontag, 1998). The gain margin represents system robustness against varying gains in the control path and the disc margin represents system's robustness to dynamical uncertainties (Sepulchre et al., 1997).

The nonlinear robustness can also be designed with structured uncertainties. In this case, the system is modeled as a set of state-space models with uncertain parameters with known bounds (Freeman and Kokotović, 1996). The robust nonlinear state-feedback and the corresponding Lyapunov function is then designed based on these uncertain models. The nonlinear control defined in this way guarantees the worst case stability within the predefined bounds for the uncertain parameters. The parameters themselves can be static, linear or nonlinear or even only known to have some bounded growth rates with known bounding functions (Freeman and Kokotović, 1996). The unmeasured uncertainties can also be rejected by augmenting the controller with an observer that indirectly measures the uncertain parameters (Krstic et al., 1995). This method defines an adaptive control for an uncertain system.

There are also other robust control design methods based on nonlinear optimal control theory. An example is dissipativity theory which used to define  $\mathcal{L}_2$  gain optimal control. The robustness comes from the closed loop system having the gains from disturbance to input and from disturbance to output bounded by the  $\mathcal{L}_2$  norm with value  $\gamma > 0$  (Van der Schaft, 1992; Sepulchre et al., 1997).

### **2.1.3 Sliding mode control**

Sliding mode control is a method where a discontinuous control signal is used to drive the system's states into a desired trajectory in the state-space. The trajectory is designed as a boundary between different states of a discontinuous switching input signal. When the boundary, or switching surface is reached, sliding motion takes place and the corresponding trajectory slides along the switching surface. (Utkin, 1977)

The discontinuous signal can also be placed in the higher derivatives of the switching function, in which case the system is called second or higher order sliding mode control depending on how many times the discontinuity is integrated to the physical control signal. Second and higher order sliding mode controllers allow continuous signals to be used in the plant excitation instead of discontinuous switched signals. (Bartolini et al., 1998; Levant, 2001)

The robustness of sliding mode control comes from the sliding manifold, which can provide a guaranteed performance for any disturbances with bounded derivatives. This allows for construction of control laws that are insensitive towards any model uncertainties that result in bounded disturbances. During sliding mode, the surface defines completely the closed loop system dynamics and ideally blocks disturbances and modeling errors that enter the system through the same state as the control. (Shtessel et al., 2013)

### **2.1.4 Internal Model Control and disturbance rejection control**

The internal model control, or IMC, is also commonly referred as robust control. The basic principle is that the system is modeled and the inverse dynamics of the model is used to provide a separation of disturbances and system state measurements (Brosilow and Joseph, 2002). If the model is perfect, then the external disturbances are com-

pletely separated from the measurement of actual states and can be attenuated directly. Although model errors are always present, partial compensation of disturbances is still achieved.

The ability to separate disturbances from the system states allows the implementation of distinct disturbance rejection control. The disturbance rejection can also be achieved with the use of disturbance observer, which is conceptually very close to internal model control as both methods are used to separate disturbances from measurements. Disturbance observer can be designed separately regardless of the used control method. (Li et al., 2014)

### **2.1.5 $\mathcal{H}_\infty$ control**

The  $\mathcal{H}_\infty$  control gets its name from the corresponding mathematical framework, where the infinity norm represents the maximum gain of a transfer function. The  $\mathcal{H}_\infty$  control is a linear control method where the maximum value of the system gain is minimized simultaneously from disturbances and some designer specified error signals (Doyle et al., 1989). Robustness is specified as bounds for perturbations of the plants dynamics which still maintain closed loop stability. The actual control design has multiple different architectures that allow the control design to adapt to different kinds of problems.

## **2.2 Robust control design methods**

Robustness is a property that all feasible control systems must possess. It has been shown that nonlinear methods outperform linear control laws, for example, when the system is nonlinear or has bounded states or inputs (Haddad and Chellaboina, 2008). Nonlinear Lyapunov based control methods are also appealing because of the fact that

the system's nonlinear dynamics and uncertainties are directly used for designing the control law which reduces over-parametrization and conservatism of the designed control law (Freeman and Kokotović, 1996). When a nonlinear plant is controlled with linear control, the nonlinearities are usually treated as uncertainty and noise to which the resulting control law is made less sensitive (Skogestad and Postlethwaite, 2007). This might make the linear controller more conservative than a corresponding nonlinear control law, especially if the nonlinearity is well known (Haddad and Chellaboina, 2008).

Downside of using nonlinear methods is the lack of systematic design tools. This is especially true with Lyapunov based methods, for which no analytic methods for Lyapunov function construction exist. The lack of systematic design tools can make nonlinear control theory difficult to employ in practical control designs. If the system under control can be transformed via state transformations, variable changes and state transitions to proper forms, specific semi systematic nonlinear control design methods can be employed. Most notable such a method is backstepping which is extendable to defining robust controllers. (Freeman and Kokotović, 1996)

Nonlinear optimal control problems can be defined using HJB equations. The steady-state solution to the HJB equation is a Lyapunov equation to the controlled system (Sontag, 1998). Optimal control is one that minimizes some defined cost function. Cost functions, that penalize the use of inputs and states, can be used to define tuning methods for the control design (Haddad and Chellaboina, 2008). The main difficulty with nonlinear optimal control is that the HJB equations are very difficult to solve (Freeman and Kokotović, 1996; Sontag, 1998).

Due to the difficulties with solving HJB equations, nonlinear optimal control design is accomplished by inverse construction of the control law. Inverse solution is obtained by first defining a function, which is then shown to be the solution to some meaningful HJB equation. (Haddad and Chellaboina, 2008)

In comparison to the difficulties in solving nonlinear control laws, the cost functions associated with linear control are solutions to Riccati equations (Marshall and Nicholson, 1970). For example, the  $\mathcal{H}_\infty$  control problem can be solved from algebraic Riccati equations (ARE) (Glover and McFarlane, 1989) . Compared to the difficulties with corresponding nonlinear HJB equations, the ARE can be solved programmatically and the algorithm can be guaranteed at least quadratic convergence (Arnold and Laub, 1984). The  $\mathcal{H}_\infty$  control theory is very mature and there are tools to automate the design process, which ease the theory's application to practical situations (Skogestad and Postlethwaite, 2007). Linear control theory in general holds a significant advantage over nonlinear theory in that linear problems are solvable and commercial software are available specifically for these purposes.

### **3 Control Design Considerations**

The need for feedback compensation comes from uncertainty in the mathematical model. If a system is perfectly known, a proper control signal can be calculated a priori and used to perfectly set a system into desired state. Typical feedback compensations like PID controller work as the the system is driven into a stationary operating point by using the error between a measurement and reference as the control input. If the system under control is stable, an integrator in the feedback loop will drive the system into zero error state assuming that the uncertainties are constant. With time varying uncertainties the integrator of a PID controller can deteriorate the systems performance (Li et al., 2014). When control is designed especially for the disturbances, the corresponding design is referred as disturbance rejection control.

Disturbance rejection can be accomplished through feedforward design, with either measured or observed disturbances. A fundamental property of linear control design is the separation principle, which states that observation and feedback are separate design problems (Luenberger, 1964). This indicates that the disturbances can be observed without effecting the nominal performance if the disturbances can be modeled as observable states in the state-space design and the corresponding augmented state is observable (Li et al., 2014). In this case, the disturbance rejection can be accomplished even without separate measurement for the disturbance.

#### **3.1 Classical robust design**

Classic measures for robustness are gain and phase margins, that measure the controlled system's tolerance to dynamic and static uncertainty. Phase margin is an indication that the system can withstand phase lag that slows down the system's operation. Gain margin implies that the system can have static uncertainty, which appears as an

uncertain gain in the loop.

The problem with gain and phase margins is that although they guarantee system's stability as long as  $GM > 0$  and  $PM > 0$ , alone they do not give a good impression on how much uncertainty is tolerated. Uncertainty in the pole and zero locations changes system's phase and gain. Most critical frequency range is in the frequencies of the open loop crossover region where system's gain drops below 0 dB. (Skogestad and Postlethwaite, 2007)

To further evaluate system's frequency-gain performance, typically a sensitivity analysis is performed. Sensitivity analysis consists of analyzing sensitivity  $S$  and complementary sensitivity  $T$  functions.  $S$  and  $T$  are defined as the transfer functions between control signal and reference and transfer function between reference and output. From the Figure 3.1, we can see that the control signal and reference can be defined as

$$u = r - y \quad \rightarrow \quad y = r - u \quad (3.1)$$

$$y = u(KG). \quad (3.2)$$

Substituting (3.1) into (3.2) gives

$$r - u = u(KG) \quad (3.3)$$

$$r = u + u(KG) \quad (3.4)$$

$$r = u(I + KG), \quad (3.5)$$

which yields the transfer function from reference to control

$$\frac{u}{r} = (I + KG)^{-1} = S, \quad (3.6)$$

and the complementary sensitivity function is defined as the transfer function from  $r$  to  $y$ . The transfer function can be obtained by substituting (3.1) into right hand side of (3.2)

$$y = (r - y)(GK) \quad (3.7)$$

$$y = r(GK) - y(GK) \quad (3.8)$$

$$y(I + GK) = r(GK) \quad (3.9)$$

$$\frac{y}{r} = (I + GK)^{-1}GK = T, \quad (3.10)$$

where  $G$  is the plant and  $K$  is the controller.

Sensitivity analysis provides the designer with the information on how well the system will tolerate dynamical errors in modeling in different frequency ranges (Skogestad and Postlethwaite, 2007). The basic idea is that the controller dominates the closed loop gain where good regulation is desired and has a gain roll-off beyond the closed loop bandwidth. This type of controller allows the feedback to compensate modeling errors and exogenous disturbances by having large control signals if the sensitivity function gets small values in the frequency range of the disturbance. For example, if a multiplicative uncertainty  $\Delta$  at given frequency is much smaller than the loop gain, then it can be seen that

$$y = r \frac{K\Delta G}{1 + K\Delta G} \approx r \frac{KG}{1 + KG} \approx r \quad (3.11)$$

If the possible uncontrollable modes are stable, and a nominal model of the plant is known with some estimates on the system's uncertainty, the sensitivity analysis can be effectively used to define and analyze control (Goodwin et al., 2001).

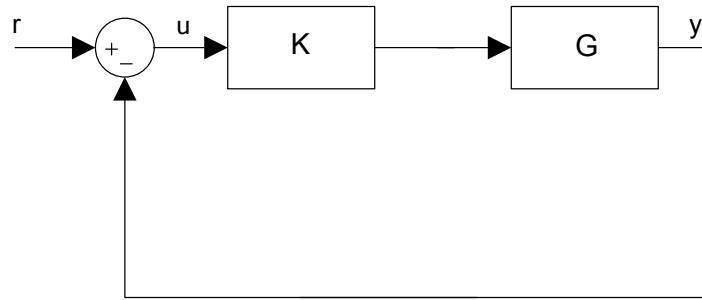


Figure 3.1. Basic feedback construction of plant  $G$  and controller  $K$ .

### 3.1.1 Control construction based on sensitivity analysis

Designing a controller based on sensitivity analysis is a very effective way for profiling a controller prior to possibly lengthy simulations. Problem with such a design method is that with plants that have complicated dynamics providing a stable controller can be difficult. Also care needs to be taken to provide the open loop system a reasonable phase response. Sensitivity analysis can be used to define a robust controller, but there is a lot of degrees of freedom left for the designer. Automating the construction of the controller by the use of optimization is highly desirable, as the optimal control method works as an abstraction layer to the control design. The control engineer uses this higher level of abstraction during design to limit the choice of analyzed controllers to those which have some desirable factors guaranteed by the design method.

Since the closed loop system is assumed to be linear, the exogenous noises do not destabilize the system as the poles of system determine its stability. However, if not taken into account noise and disturbance signals can be catastrophic to the overall performance. The limits of achievable gain slopes also limits the loop shaping controller filtering capabilities. The controller has quite wide transition band from disturbance rejection to noise rejection as the gain roll off can not be practically higher than  $-40$  dB/dec (Vinnicombe, 2000).

Usually the noise is in high frequency and it can be further attenuated with addition of a loop filter. The basic feedback construction with loop filter  $F$ , disturbance and noise is

shown in Figure 3.2. Although the loop filter does attenuate noises, it also introduces phase shifts than can deteriorate the system's performance further (Goodwin et al., 2001). The classic solution to this problem is the LQG design which is a special

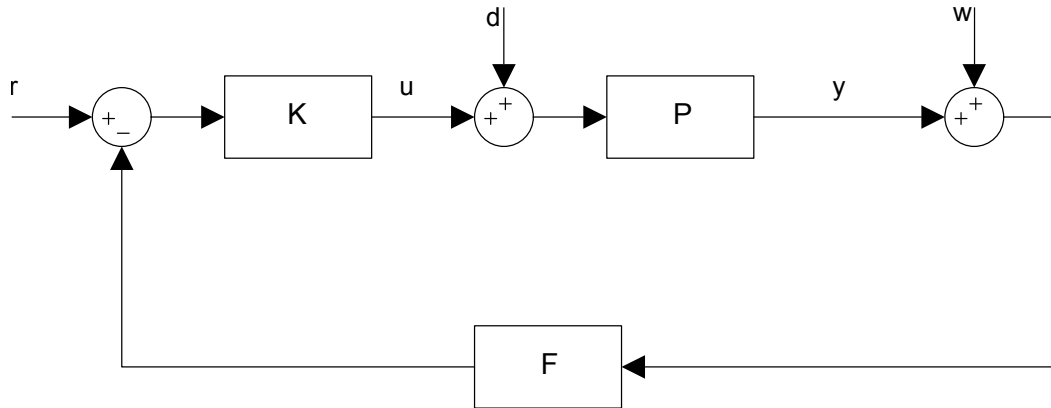


Figure 3.2. Basic feedback construction with different disturbance and noise signals shown with loop filter  $F$ .

case of  $\mathcal{H}_2$  optimal design (Skogestad and Postlethwaite, 2007) (Doyle et al., 1989). However, the LQG controller has problems with stability as discussed by (Doyle, 1978) and (Glover and McFarlane, 1989).

Optimal control design based on the direct minimization of sensitivity function can be used, but it is shown for example in (Vinnicombe, 2000) be excessively susceptible to pole placement of the nominal model. Without any extra parametrization of usable control signals, the direct minimization of sensitivity function would also place all the poles to infinity if system does not have delay or non-minimum phase dynamics limiting the controller bandwidth. More convenient way to define an optimal controller for a plant was described in (Glover and McFarlane, 1989). The idea is to modify the open loop shape of the controllable system instead of the sensitivity functions directly, to obtain desired performance and use the  $\mathcal{H}_\infty$  controller to stabilize the shaped design.

## 4 Overview of loop shaping $\mathcal{H}_\infty$ control design

Robustness against model uncertainties is one of fundamental design goals of control design. Linear robust control that allows model uncertainty can be designed using the  $\mathcal{H}_\infty$  framework. The name comes from the used mathematical framework, the Hilbert space, that is bounded by the infinity norm. This corresponds to a space of stable real valued rational functions with bounded gains, meaning a linear real valued transfer function with the poles in the open left half plane. The infinity norm of a transfer function is the maximum absolute gain, formally defined as

$$\|G(s)\|_\infty = \sup_{u \neq 0} \frac{\|y\|_2}{\|u\|_2}, \quad (4.1)$$

where  $u$  is the input signal, and  $y$  output signal.

The  $\mathcal{H}_\infty$  control is designed to create the controller  $K$  directly to minimize some designer defined transfer functions such that the infinity norm of the closed loop system gain has some finite value. Thus the system has its output bounded if the input is of finite energy i.e.  $\|u\|_2$  exists. The  $\infty$ -norm is therefore a logical choice for improving systems robustness, since it is a measure for system's maximum gain given that the input signal is 2-norm bounded. As is noted in (Vinnicombe, 2000), the typical sine, step and ramp signals are neither of finite energy nor have bounded 2-norms, however the use of  $\infty$ -norm still makes sense since all finite signals have bounded energy in a finite interval.

The guaranteed robustness against modeling errors is achieved by formulating the control design problem in a way that the designed controller bounds the infinity norm of some nominal model with some allowable set of perturbations. One method for defining the uncertainty set is by coprime factorization of the nominal model and with additive uncertainty acting on the coprime factors (Glover and McFarlane, 1989). The coprime factorization of a system  $G$  is done by defining polynomials  $N$  and  $M$  such

that

$$G = N^{-1}M. \quad (4.2)$$

The uncertainty can be represented by stable perturbations  $\Delta_N$  and  $\Delta_M$  added to the nominal system so that the uncertain model can be represented as

$$G_P = (N + \Delta_N)^{-1}(M + \Delta_M). \quad (4.3)$$

The goal of the control design is to provide a controller that stabilizes the set of plants defined by

$$G_P = \{(N + \Delta_N)^{-1}(M + \Delta_M) : \|\Delta_N, \Delta_M\|_\infty < \epsilon\}, \quad (4.4)$$

and  $\epsilon$  is the stability margin (Glover and McFarlane, 1989).

#### 4.1 Stabilizing $\mathcal{H}_\infty$ control

The standard representation for robust control synthesis is done with a plant represented with error, state and control signals with the plant partitioned as

$$\begin{bmatrix} z \\ y \end{bmatrix} = \underbrace{\begin{bmatrix} P_{11} & P_{12} \\ P_{21} & P_{22} \end{bmatrix}}_{P(s)} \begin{bmatrix} w \\ u \end{bmatrix}, \quad (4.5)$$

where the signals  $z, y, u$  and  $w$  are the error signals, measurements, the input and exogenous signals, such as disturbances and noises. The plant  $P$  maps the state and measurement signals to input signals. The controller is to be defined is one that simultaneously minimizes the  $\infty$ -norm of the transfer functions from  $[z, y]$  to  $[w, u]$  such that the stability is simultaneously guaranteed for a set of additive uncertainty affecting coprime factors of the system.

#### 4.1.1 State-Feedback form of stabilizing $\mathcal{H}_\infty$ controller

The robust stabilizing controller has an exact state-feedback structure, which allows its implementation as a standard state-feedback and observer form. The generalized transfer matrix in (4.5) has state equation of the form

$$P = \left[ \begin{array}{c|cc} A & B_1 & B_2 \\ \hline C_1 & D_{11} & D_{12} \\ C_2 & D_{21} & D_{22} \end{array} \right], \quad (4.6)$$

where the disturbance input is determined with the  $C_1$  matrix and the measurements enter through the  $C_2$  matrix. The D matrices determine inputs and corresponding input disturbances coupling to the output. The plant  $(A, B, C, D)$  is partitioned with  $A = A$ ,  $B = [B_1, B_2]$ ,  $C = [C_1, C_2]^T$ ,  $D = \begin{bmatrix} D_{11} & D_{12} \\ D_{21} & D_{22} \end{bmatrix}$ .

A specific solution to the  $\mathcal{H}_\infty$  control problem for the above plant can be obtained using state feedback and observer gains of the form

$$K = -S^{-1}(D^T C + B^T X) \quad \text{and} \quad L = -(BD^T + ZC^T)R^{-1},$$

where  $R = I + DD^T$  and  $S = I + D^T D$  (McFarlane and Glover, 1988). The variables  $X$  and  $Z$  are obtained by solving two algebraic riccati equations that are referred as *generalized control algebraic riccati equation* (GCARE) and *generalized filter algebraic riccati equation* (GFARE) (Glover and McFarlane, 1989). The riccati equations are defined as

$$(A - BS^{-1}D^T C)^T X + X(A - BS^{-1}D^T C) - XBS^{-1}B^T X + C^T R^{-1}C = 0 \quad (4.7)$$

$$(A - BS^{-1}D^T C)Z + Z(A - BS^{-1}D^T C)^T - ZC^T R^{-1}CZ + BS^{-1}B^T = 0, \quad (4.8)$$

where (4.7) is the GCARE and (4.8) is GFARE. Interestingly the observer of the  $\mathcal{H}_\infty$  controller is the solution to the associated  $\mathcal{H}_\infty$  filtering problem (Doyle et al., 1989). The maximum achieved stability margin is given in (Glover and McFarlane, 1989) as

$$\epsilon_{max}^{-1} = (1 + \rho(XZ))^{\frac{1}{2}} \quad (4.9)$$

where  $\rho$  represents maximum eigenvalue and  $X$  and  $Z$  are solutions to the GCARE and GFARE.

With the stabilizing state controller and observer, the closed loop has the standard representation which in state equation form is

$$\begin{aligned} \dot{x} &= Ax + Bu_c \\ u_c &= K\hat{x} \\ \dot{\hat{x}} &= A\hat{x} - L(C_2\hat{x} - y) + Bu_c \end{aligned} \quad (4.10)$$

and  $u_c$  is the controlled input signal,  $A, B, C$  and  $D$  the system matrices and  $L$  and  $K$  controller gains as stated in (4.1.1). The design of  $\mathcal{H}_\infty$  controller is done by properly designing the plant in (4.6) and the controller is obtained by solving the riccati equations (4.7) and (4.8). This design guarantees that the resulting system is stable in the face of uncertainty that can be modeled as stable perturbations on the coprime factorized plant but it does not provide means to design closed loop system performance. The performance can be designed by additional design step of incorporating a weighing function for the open loop shape (McFarlane and Glover, 1992).

## 4.2 Loop Shaping $\mathcal{H}_\infty$ controller

The procedure for modifying the performance of stabilizing  $\mathcal{H}_\infty$  controller has two parts, designing a weighing function for attaining desirable open loop shape and obtaining the robust controller to stabilize the weighed plant. Generally the designer

chooses the loop shape to have close to  $-20$  dB/dec slope of the gain in the crossover region and higher roll off in higher frequencies to further reduce the effect of high frequency noises (Skogestad and Postlethwaite, 2007). Most often the controlled frequency region is the low frequency range hence the controller in which case the controller is augmented with an integrator to push the DC gain of open loop to infinity. The further poles and zeros are placed to have ideally steeper gain in low and high frequencies to maximize the low frequency gain and minimize the high frequency gain. In practice, the maximum achievable gain slopes are limited by the phase to around  $-40$  dB/dec (Skogestad and Postlethwaite, 2007) (Vinnicombe, 2000).

When the desired loop shape is obtained the open loop plant is partitioned to the form in (4.6) by augmenting the plant with the loop shaping function and the robust controller is solved from GCARE and GFARE.

## **5 Switch-mode power supply control**

The energy that is fed through a switch mode converter, is controlled by varying the input voltage of a converter. The input voltage is commonly controlled with pulse width modulation, but other modulation methods are also available, like phase-shift and frequency modulation (Erickson and Maksimovic, 2001).

The manipulated control variable is referred as the duty ratio, which represents the ratio on conduction time to the whole switching cycle. Duty ratio is commonly thought of being purely rectangular, which means that the average voltage over one cycle of switching action is the supply voltage multiplied by the duty ratio. This makes the switching converter behave like a variable voltage input to the controlled system (Wester and Middlebrook, 1973).

Since the input voltage to the system is applied through the manipulation of switch conduction times, the control action can have arbitrarily fast changes between control cycles as pulse width can vary from allowable maximum to minimum between two consequent cycles. Such a control is typically not attainable, but there are no limitations to the control signal speed posed by the controllable plant itself. This is contrary to most physical processes, like chemical or mechanical processes, where high frequency control action causes wear in the equipment like valves, joints and other moving parts of a system.

### **5.1 Limitations of switching converter control**

Because the control speed is not limited by the manipulated actuator, the switch mode supplies are commonly controlled with as fast control as possible. The limitations of the speed come from the switching frequency, dimensioning of the reactive components and supply voltage which are explained next.

### **5.1.1 Switching frequency**

The switch mode modulation makes the system behave like a sampled system and therefore limits the maximum bandwidth attainable by control to less than half of the switching frequency (Erickson and Maksimovic, 2001). The switching frequency is generally limited by increase of losses present in the circuit (Onodera et al., 1981). The major contributors to losses that are increased with switching frequency are the finite switching times, the gate charge of the switches and copper and core losses in inductors and capacitors (Onodera et al., 1981).

### **5.1.2 Digital calculation cycle**

When digital control is applied, it is also possible that the converter needs to be controlled with lower frequency control cycle than that of the switching frequency. This is because either the higher speed control does not improve the attainable control bandwidth, or it is not economical in sense of the required processing power of the control unit. In this case, the digital control calculation cycle might also be a factor that limits the attainable control bandwidth due to increased phase shift associated with lowering the sampling frequency. (Åström and Wittenmark, 2011)

### **5.1.3 Limitation by bounded states**

It is also fairly common that the control needs actively to limit some states from growing beyond allowable ranges. The ranges are determined by safe operation area of the circuit's currents and voltages or measurement ranges. The hard bounds to inputs and states limit the maximum speed of the control when the control would otherwise make the input or state variables higher than allowed by the saturation. (Brosilow and Joseph, 2002)

#### 5.1.4 Unstable zero dynamic

Current fed converters are typically nonlinear and can have non-minimum phase dynamics for some of the states. Converters falling into this category are, for example, Cúk, SEPIC, boost and Buck/Boost converters (Erickson and Maksimovic, 2001). The non-minimum phase dynamic is a fundamental limitation of the achievable bandwidth for that specific state and cannot be mitigated by feedback control (Goodwin et al., 2001; Skogestad and Postlethwaite, 2007).

The zero dynamic cannot appear in all states and the overall control of the system can be made fast with the use of extra measurements and feedforward control. The existence of non-minimum phase dynamic does make the affected state have undershoot, and in case of imaginary unstable zeroes oscillations, that are made worse when system speed is increased. The undershoot and oscillations might also be a limiting factor when the system control is designed as they might cause some of the states to exceed their maximum allowable ranges. (Brosilow and Joseph, 2002)

## 5.2 Robust control of phase shifted full-bridge buck converter

In this section, a robust control of a phase shifted full-bridge buck converter is presented. The converter is controlled via cascade control where inner current loop is designed using the  $\mathcal{H}_\infty$  control design method and the voltage loop is controlled with a simple PI -controller. Voltage is not controlled using a single loop because of the need for active current limit in case of overload. In order to lighten the notation, the phase shifted full-bridge buck converter will be referred as HB or HB-converter, as in H-bridge converter, hereinafter.

The plant under control is presented in Figure 5.1. The converter is a full bridge buck converter with added primary series inductance and current doubler secondary. The

primary series inductance is used to widen the range of input current that ensures of zero-voltage switching(ZVS) at high voltage side switch turn on. The secondary rectifier low side diodes are replaced by synchronously switched mosfets for minimizing the conduction losses in the secondary side and the high side switches are replaced by inductors. The current doubler is redrawn in Figure 5.2 as full bridge rectifier with inductors in place of high side semiconductors for the sake of clarity. The HB converter

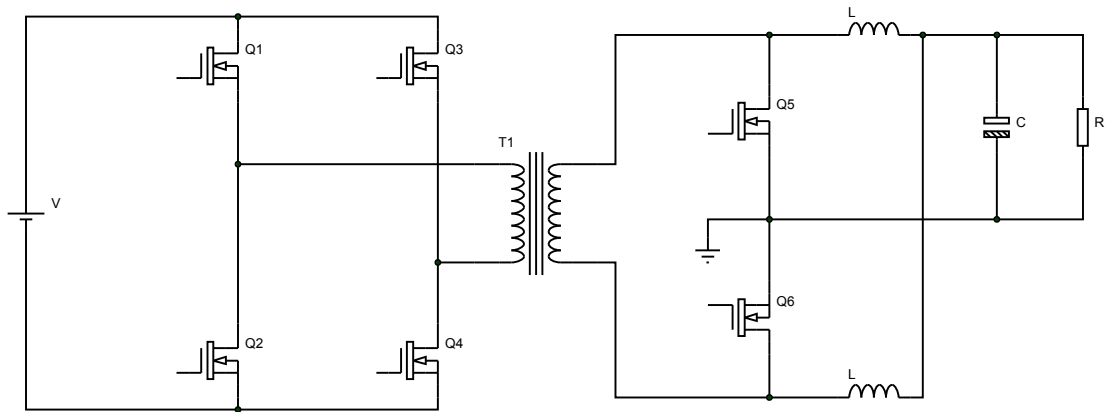


Figure 5.1. Phase shifted full bridge converter with current doubler rectifier secondary.

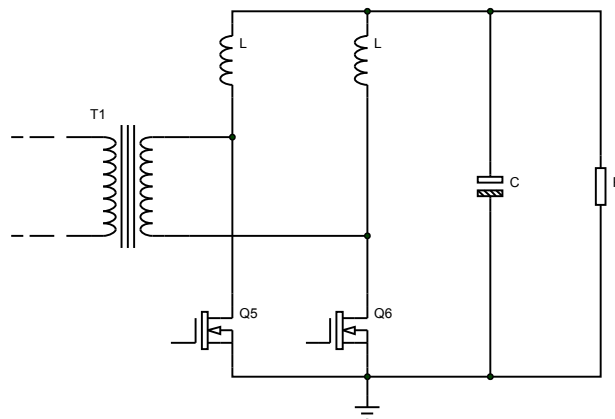


Figure 5.2. The current doubler rectifier drawn as a bridge with high side inductors.

switches are controlled with phase shift modulation, in which the legs are switched at 50 % duty ratio and the the voltage across the transformer primary is controlled by the phase shift between the legs (Redl et al., 1990). The phase shift modulator implements actively clamped zero-vector which preserves the inductor current and thus allows for zero voltage state at switch turn on. At turn on, the circulating current discharges the conducting switches inherent capacitances. This happens during switch transition and

since the voltage does not change instantaneously, voltage across the switch is low during the transition, hence near zero voltage turn on is achieved. Turnoff is still hard switched. In secondary, the voltage waveform is typical square pulse. The detailed operation of phase shifted full bridge is given in (Redl et al., 1990)

The system is modeled in state-space. Even though the system has two distinct output inductors, the state-equation is simplified to only model the dynamic based on single inductor. The model of the current doubler full bridge buck converter is presented exhaustively in (Cao, 2007). Although the converter has two output inductors, the waveforms are identical and thus the currents of the inductors are even in practical circuit are very close to each other. Because of the similar currents, the output inductors can be accurately modeled as a single inductor with the combined current. The state-space model of the system is

$$\dot{x} = \begin{bmatrix} -\frac{R_1}{L} & -\frac{R}{R_2 L} \\ \frac{R}{CR_2} & -\frac{1}{CR_2} \end{bmatrix} u + \begin{bmatrix} \frac{V_{in}}{nL} \\ 0 \end{bmatrix} d, \quad (5.1)$$

$$x = [i_L, v_c]^T,$$

$$u = d,$$

where the resistances  $R_1$  and  $R_2$  are

$$R_1 = R_{eq} + \frac{R_{es}R}{R_{es} + R}, \quad (5.2)$$

$$R_2 = R + R_{es}, \quad (5.3)$$

and the  $R_{es}$  is the capacitor equivalent series resistance and  $R_{eq}$  is the equivalent series resistance that models the voltage loss of the ZVS switching condition. The ZVS voltage loss equivalent resistance is defined as

$$R_{eq} = \frac{2L_k f_t}{n^2} \quad (5.4)$$

Even with the ZVS condition, the phase shifted full bridge exhibits linear behavior, as the only variable in the ZVS voltage loss  $R_{eq}$  is the state  $x_1$  assuming that sourcing voltage  $V_{in}$  is constant.

### 5.2.1 Dynamic behavior

The HB-converter can be seen to have similar state-equation to regular buck converter. The continuous current buck converter is strict minimum phase and linear, which makes up for simple controllable dynamic. The difference comes from the ZVS property of the primary side. The ZVS switching reduces the apparent voltages available with increasing current. This makes the phase shifted converter behave as if it had significant input impedance as the voltage available to secondary is reduced with increased load current at given pulse width. This effect is modeled as a resistance that depends on the transformer leakage inductance, inductor current and operational frequency.

The current measurement of the HB-converter is in the primary DC-link side. The current measurement is synchronously sampled with sampling instant timed to the peak at the edge of the current pulse. The peak current of the waveform depends on the converters switching mode (ZVS vs hard switching), the input and output voltages and the loading of the system. The dependance of current measurement on system states makes the converter exhibit slight nonlinear behavior in the measurement. Although the current of the inductors are not directly measured, the DC-link measurement is effectively just scaled version of the inductor current and the nonlinear behavior was determined in the laboratory measurements to be of no concern.

The control cycle is set at 50 kHz. The control cycle is limited to less than switching frequency as there is a need to conserve calculation resources of the processor. In addition to the control of the full bridge converter, the same processor is also used to

control of a power factor correction, handle data logging, communication and various other functions like condition monitoring.

### **5.2.2 Control objectives**

The overall power converter is designed to be a single phase mains fed converter with 24 V output voltage. The grid is interfaced with active power factor correction which regulates the DC-link voltage to nominal 400 V. The 400 V DC-link is regulated to 24 V with the introduced full bridge phase shifted converter.

The phase shifted converter is specified to work from open load to overload conditions. The system can also be loaded with power load, which is a destabilizing perturbation to the nominal operation of the converter. During overload condition the power supply is designed to output the maximum current. The system has measurements from DC-link voltage and current and output voltage and current.

The controller needs to provide steady output voltage in the presence of load and input voltage perturbations. Due to the overload operation the controller is designed as cascaded voltage and current controllers, where the outer loop voltage controller's output is the current reference. The voltage controller therefore can be considered as a virtual controller as its output is not the actual control signal. The current controller is designed as the inner control loop and it feeds the modulator with the actual control signal which is realized as switchings.

The converter is natively in the cascade form which makes it suitable for applying cascade control. Single loop control could possibly perform better, but the cascade structure allows for simpler implementation of saturation functions for maximum both, current reference and duty cycle. Furthermore, the measurements from output current and input voltage allow feedforward compensation of load (Kanemaru et al., 2000) and

input voltage disturbances (Kelkar and Lee, 1983).

Because of the requirement of robust current control, the current controller is designed using the robust control methods. The importance of the current controller is to provide a well regulated inner loop, so that the possible outer loop can be designed using a simplified dynamical system. In this case the current controller effectively acts as controlled current source, hence the resulting voltage dynamic is first order linear system. The robust control methods are therefore used only on the current controller.

In order to limit the discussion to just the robust control methods, only the current loop control design is presented with measurements.

### **5.2.3 Robust control design for current loop**

$\mathcal{H}_\infty$  controller is designed using the loop shaping method that was introduced in (McFarlane and Glover, 1988). The method consists of modifying the the open loop singular values using weight functions to yield satisfactory open loop response. Since the system is scalar, the singular values are the same as the systems gain and the absolute gain value of the transfer function can be used to design the loop shape. The principles of regular loop shaping is used and the gain slope is designed to be close to -20 dB/dec at crossover frequency with higher slope at higher frequencies and high gains at lower frequencies. This allows the system to track references and attenuate high frequency noises.

The system parameters for the model (5.1) are

Constant	Description	Value
$R$	load resistance	240 m $\Omega$
$C$	output capacitance	27.3 mF
$L$	inductor value	15 $\mu$ H
$ft$	switching frequency	60 kHz
$R_{es}$	capacitor ESR	1.3 m $\Omega$
$R_{eq}$	equivalent source resistance	20.9 m $\Omega$
$n$	transformer winding ratio	9.7

This corresponds to a transfer function

$$P(s) = 1.9284 * 10^6 \frac{s + 151.8}{s^2 + 1633s + 2.64 * 10^6}, \quad (5.5)$$

which puts complex pair of poles at 1624.9 rad/s.

Since the system is needed to track a current reference, the controller is first appended with an integrator. The integrator induces phase lag, therefore a zero is placed on relatively low frequency at 500 rad/s to counter the lag.

The equation also has a low frequency zero, which makes the system exhibit overshoot in current dynamics. This low frequency zero is compensated by placing a pole close to it and lastly weight function is scaled to yield an open loop crossover frequency in the range of 5 kHz. The final weight function is chosen as

$$W1(s) = 0.224 * \frac{s + 500}{s} * \frac{s + 2170}{s + 180} \quad (5.6)$$

The  $\mathcal{H}_\infty$  controller is then obtained by solving the associated robust control and filter Riccati equations where the matrix elements are a combination of the plant and the weighing function, as described in chapter 4. The noise and disturbance channels  $C_1$  and  $[D_1, D_3]$  are chosen as unity and the corresponding state-space equation is padded

with zeros to obtain properly defined system. The filter and gain matrices are

$$K_{\infty} = \begin{bmatrix} -0.1919 \\ 0.2930 \\ -3.7542 \\ -1626.6 \end{bmatrix}^T, \quad L_{\infty} = \begin{bmatrix} 4419.9 \\ 36.162 \\ 127.48 \\ 0.0029 \end{bmatrix} \quad (5.7)$$

$K_{\infty}$  is the state feedback gain and  $L_{\infty}$  the filter gain matrices. With the specified control and observer gains, the system sensitivity and complementary sensitivities are shown in Figure 5.3 with corresponding open loop bode in Figure 5.4

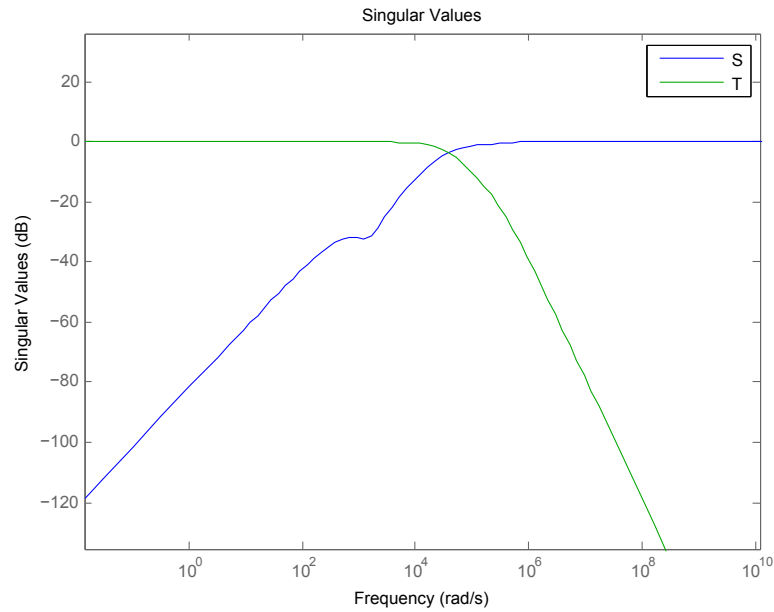


Figure 5.3. The sensitivity function  $S$  and complementary sensitivity function  $T$  of the robust loop shaping controller. The sensitivity shows no peaking of the loop shape and it can be observed that the basic notions of low sensitivity at low frequencies and low complementary sensitivity at high frequencies are fulfilled.

### 5.3 Digital control implementation

Controllers are commonly implemented by means of digital representation of the dynamics of the controller. Digital controller has analog to digital converter to sample and digitize the measurements and a digital to analog converter interfacing the digi-

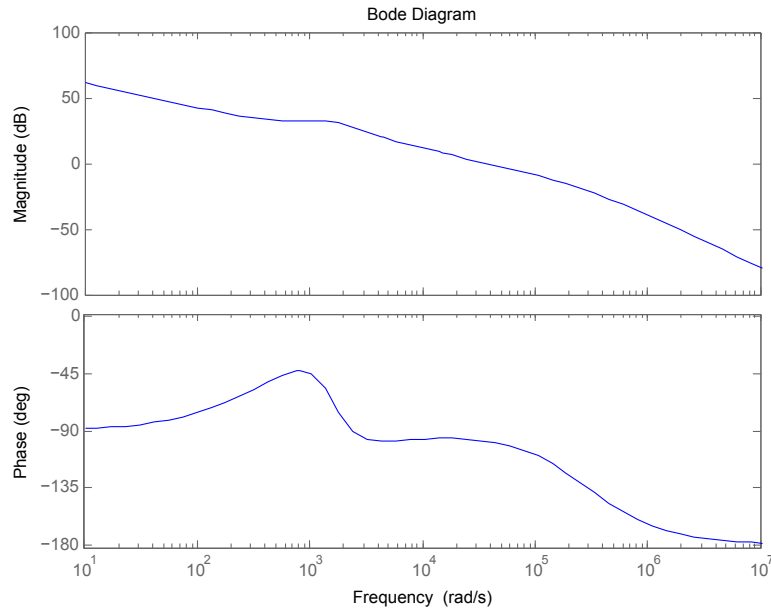


Figure 5.4. Open loop bode plot using the loop shaping robust controller. The system has cross over frequency of about 5 kHz. The gain margin is ideally infinite and phase margin of 80 degrees.

tal signals with analog circuitry. In power electronics, the modulator acts as a D/A converter, as the digital controller outputs the gate signals. Digital control can be designed in the analog domain and the digital controller is obtained by discretization of the continuous controller (Azar, 1965).

The designed robust controller has effectively three parts, the robust observer, the robust controller and the loop shaping function. The structure of the controller is shown in Figure 5.5. Since the associated digital control unit that does the computations of the controller takes finite time to execute and has finite accuracy, the structure of the controller algorithm might have significant effect on performance of the implemented controller (Åström and Wittenmark, 2011).

### 5.3.1 Control code structure

The accuracy in which the poles can be placed depends on the structure of the chosen controller and the word length in which the coefficients of the controller can be rep-

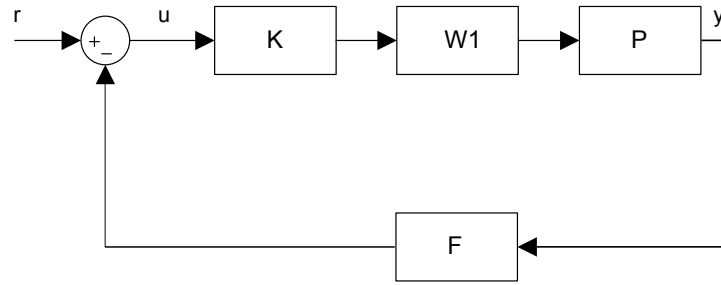


Figure 5.5. The structure of the implemented controller.  $F$  is the robust observer,  $K$  the robust controller,  $W1$  is the loop shaping function and  $P$  the plant under control.

resented. The control structure can also be optimized in conjunction with scaling of the coefficients that make up the transfer function to minimize peak noise power, the dynamic range of the coefficients and in case of fixed point calculation, the possibility of run-time register overflow.

The state matrix observer-feedback representation of the controller is computationally cumbersome, hence the controller and observer discretized using the Tustin method which are then converted to transposed direct II forms. The direct II forms require the minimum amount of operations (Proakis and Manolakis, 2007). Since the processor used is floating point, the register overflow cannot practically occur (Taylor and Mellott, 1998) and minimum dynamic range for the coefficients is chosen for the structure.

The observer and the controller can be partitioned into two transfer functions that have the order of the full plant (Goodwin et al., 2001), that is the order of the loop shaping weight plus the order of the plant. The loop shaping weight given in equation (5.6) is of order 4 and the plant is of order 2, hence the robust controller and observer are of order 6. Interestingly, such an arrangement has the poles of the forward path shown as the zeros on the feedback path and zeros on the forward path become the poles on the feedback path. This structure is shown in for example in (Vinnicombe, 2000) to be optimal in a sense that any other arrangement of the controller has smaller set of functions that it can track efficiently.

### 5.3.2 Test measurements

The system is tested in the laboratory. The measurements are taken from the digital controller, since the actual signals were not measurable from the test device. The current was measured from DC link side of the converter instead of the inductor side. The current is synchronously sampled from the peak of the current waveform. Although the system model describes the dynamics of the current in the inductors, the sampled current was found to match the model closely enough.

The controller was tested at start-up with constant current reference set for the current controller. The system has bounded minimum and maximum pulse widths. The minimum pulse causes a large start up current peaking which is uncontrollable as the input is already saturated at minimum. System is started with 500 cycles of minimum pulse width to allow the voltage to settle before the control is started. The observer was not updated during the start-up, but can be seen to converge to the real value. Lastly, the modeled and measured step responses are shown. The model has higher load, hence it has higher initial current, but they have relatively similar step responses aside from the ringing present in the actual device. The performance of the observer can be seen

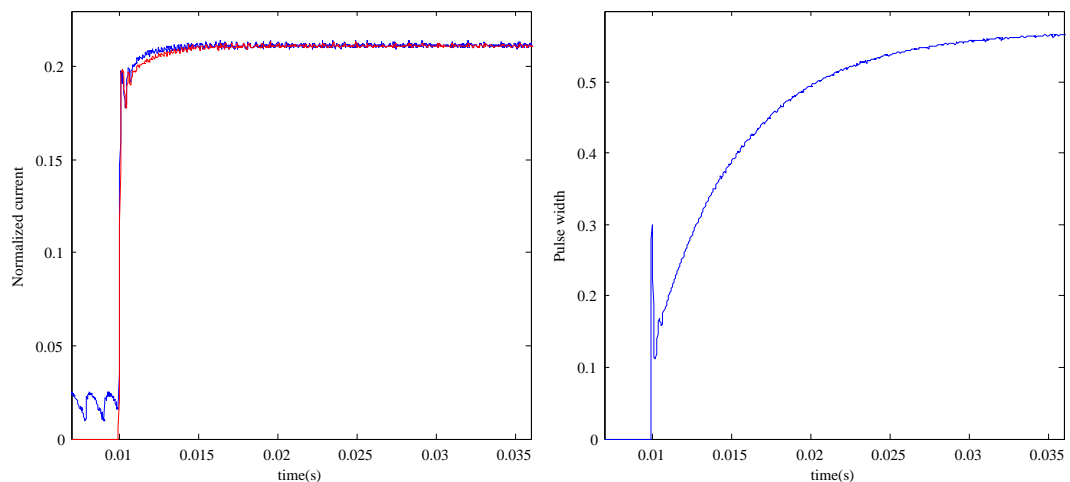


Figure 5.6. 50 A step test with the corresponding input during the step. The controller gain was tuned in the lab to get well behaved step.

in Figure 5.9 which is a close up of the 100 A and 50 A currents. The observer can

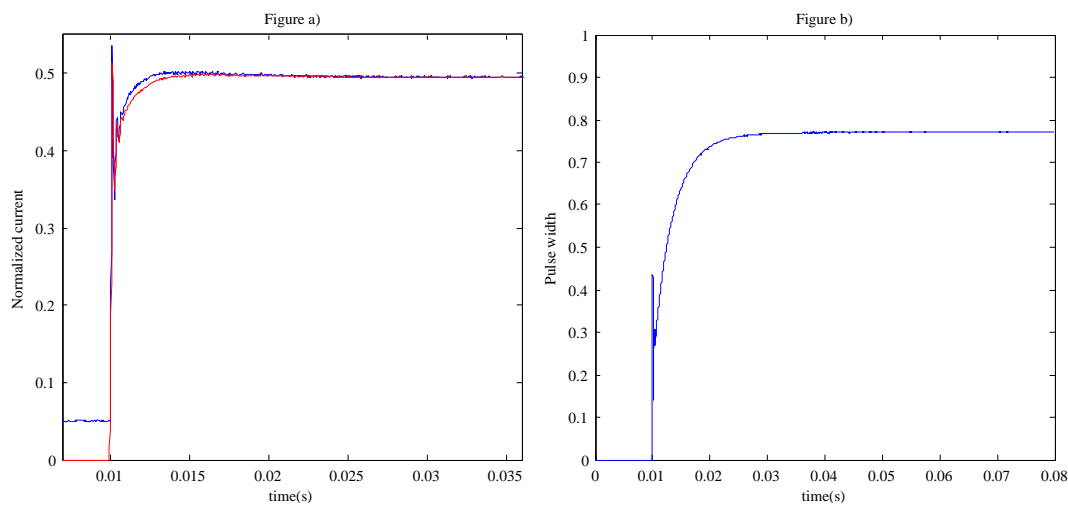


Figure 5.7. Figure a) 100 A step test and the  $\mathcal{H}_\infty$  estimate in red and Figure b. shows the input during the step. The observer is not updated during the start sequence which explains why the value is zero during first 10 ms.

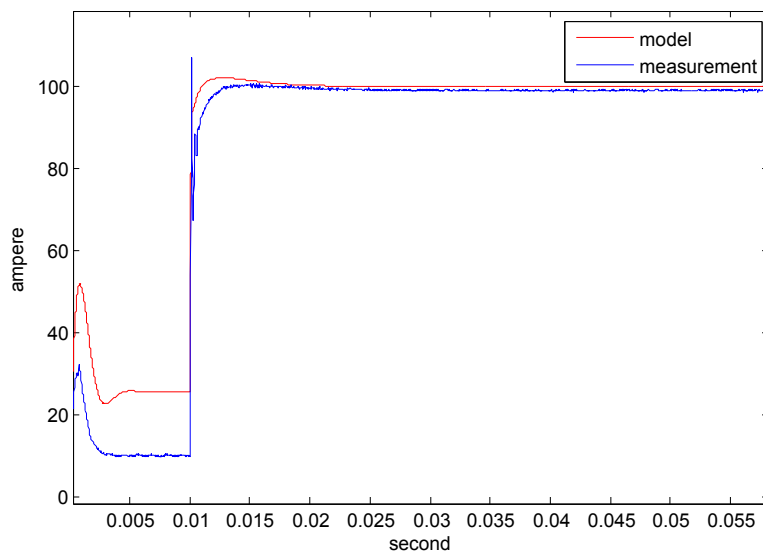


Figure 5.8. Comparison between modeled and measured step responses. Modeled step has higher initial current due to slightly higher load, but the loading does not have significant effect on the current controllers performance.

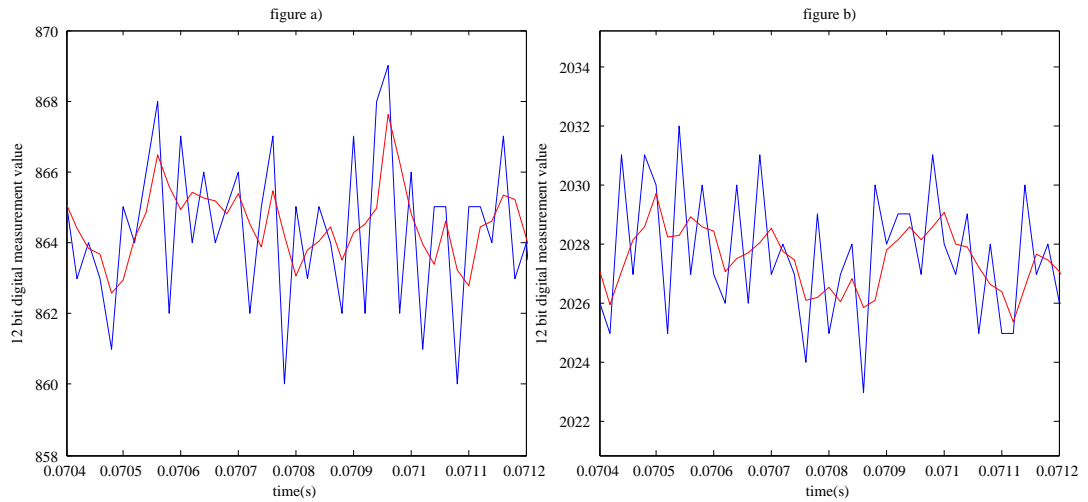


Figure 5.9. Performance of the observer during steady state operation. Figure a) shows the 50 A measurement and Figure b) the 100 A measurement. The y-axis is scaled to the digital value of the 12 bit A/D converter.

be seen to have significantly lower noise than the corresponding current measurement, which translates to smaller high frequency chattering of the input signal.

## 6 Notes and discussion

In this thesis, a robustness of control was explained and few common methods used to design robustness in control were presented and the need for robustness was also discussed. The  $\mathcal{H}_\infty$  control method was chosen over other robust methods, like robust nonlinear Lyapunov control or Sliding mode control, because of the availability of design tools. The laboratory measurements show that the implemented controller has comparable performance to the simulated model, but with additional overshoot at high current. The performance can be recovered by the use of feedforward control with either the disturbances measured directly, or indirectly via the use of disturbance observers. The tracking performance can be improved also with the use of a two degree of freedom controller.

Due to the need to handle varying loading, the proper current that stabilizes the output voltage varies. The control needs to correct the uncertainties present in the circuit, which is why high bandwidth and robustness are mandatory. Feedforward and disturbance rejection control will lessen the requirement for bandwidth as they can be tuned to affect the specific disturbances without relying on high gain feedback alone.

The architecture of the controller was chosen as cascade control, with robust inner loop current controller and regular PI controller for outer loop. This structure allows for saturation functions to be implemented for either of the two controllers. Saturation functions are needed to allow safe operation close to systems maximum safe operation range where either or both of the controllers outputs can be in saturation for prolonged periods of time. This also allows for short circuit operation, where the system behaves as a current source for the load. With the saturation operations the power supply can have guaranteed recovery from either the loss of load of the output.

The controller could have been designed to directly control the output voltage, but implementing boundaries for both the maximum current and maximum control signal

would have been more difficult. The current loop of the controller was designed using the  $\mathcal{H}_\infty$  loop shaping method.

The uncertainties associated with the plant under control were fairly well known and deriving tight bounds would have been possible, however the  $\mathcal{H}_\infty$ -control method is nonparametric towards the uncertainty in the sense of the control design. The designed control therefore very likely guarantees stability for much larger set of plants than needed and the allowed uncertainty set contains plant perturbations that are not possible. The implemented controller is likely conservative because of the allowed excessively large set of uncertainty.

The parametrized uncertainty could have been used for designing a robust control law with tighter bounds. There are numerous methods for defining control laws for specifiable set of plants. The nonlinear state-feedback based on Lyapunov functions is especially well suited for this type of robust control design since the uncertainties are measurable and has known bounds.

The choice of a robust controller that has the best dynamic in the presence of uncertainties will be a topic of future research.

## References

- Arnold, W.F., I. and Laub, A. (1984), “Generalized eigenproblem algorithms and software for algebraic riccati equations,” *Proceedings of the IEEE*, vol. 72, no. 12, pp. 1746–1754.
- Azar, Y. (1965), “Z-transforms and their applications in control engineering,” *Radio and Electronic Engineer*, vol. 30, no. 1, pp. 53–67.
- Bartolini, G., Ferrara, A., and Usani, E. (1998), “Chattering avoidance by second-order sliding mode control,” *IEEE Transactions on Automatic Control*, vol. 43, no. 2, pp. 241–246.
- Brosilow, C. and Joseph, B. (2002), *Techniques of model-based control*, Bernard M. Goodwin.
- Cao, L. (2007), “Small signal modeling for phase-shifted pwm converters with a current doubler rectifier,” in *Power Electronics Specialists Conference, 2007. PESC 2007. IEEE*, pp. 423–429.
- Doyle, J. and Stein, G. (1981), “Multivariable feedback design: concepts for a classical/modern synthesis,” *Automatic Control, IEEE Transactions on*, vol. 26, no. 1, pp. 4–16.
- Doyle, J. (1978), “Guaranteed margins for lqg regulators,” *IEEE Transactions on Automatic Control*, vol. 23, no. 4, pp. 756–757.
- Doyle, J., Glover, K., Khargonekar, P., and Francis, B. (1989), “State-space solutions to standard  $h_2$  and  $h_\infty$  control problems,” *Automatic Control, IEEE Transactions on*, vol. 34, no. 8, pp. 831–847.
- Erickson, R.W. and Maksimovic, D. (2001), *Fundamentals of power electronics second edition*, Springer.

- Freeman, R.A. and Kokotović, P. (1996), *Robust nonlinear control design state-Space and Lyapunov techniques*, Birkhäuser Boston.
- Glover, K. and McFarlane, D. (1989), “Robust stabilization of normalized coprime factor plant descriptions with  $h$  infin;-bounded uncertainty,” *Automatic Control, IEEE Transactions on*, vol. 34, no. 8, pp. 821–830.
- Goodwin, G.C., Graebe, S.F., and Salgado, M.E. (2001), *Control system design*, Prentice Hall.
- Haddad, W.M. and Chellaboina, V. (2008), *Nonlinear dynamical systems and control: a Lyapunov-based approach*, Princeton University Press.
- Kanemaru, S., Nabeshima, T., and Nakano, T. (2000), “Transient response in a buck converter with bulk decoupling capacitors employing load current feedforward control,” in *Power Electronics and Motion Control Conference, 2000. Proceedings. IPEMC 2000. The Third International*, vol. 1, pp. 258–262 vol.1.
- Kelkar, S.S. and Lee, F. (1983), “A novel feedforward compensation canceling input filter-regulator interaction,” *Aerospace and Electronic Systems, IEEE Transactions on*, vol. AES-19, no. 2, pp. 258–268.
- Krstic, M., Kanellakopoulos, I., and Kokotovic, P.V. (1995), *Nonlinear and adaptive control design*, John Wiley & Sons Inc.
- Levant, A. (2001), “Universal single-input-single-output (siso) sliding-mode controllers with finite-time convergence,” *Automatic Control, IEEE Transactions on*, vol. 46, no. 9, pp. 1447–1451.
- Li, S., Yang, J., Chen, W.H., and Chen, X. (2014), *Disturbance observer-based control: methods and applications*, CRC Press.
- Luenberger, D. (1964), “Observing the state of a linear system,” *IEEE Transactions on Military Electronics*, vol. 8, no. 2, pp. 74–80.

- Lyapunov, A.M. (1892), *The general problem of the stability of motion*, Ph.D. thesis, Kharkov Mathematical Society.
- Marshall, S. and Nicholson, H. (1970), “Optimal control of linear multivariable systems with quadratic performance criteria,” *Electrical Engineers, Proceedings of the Institution of*, vol. 117, no. 8, pp. 1705–1713.
- McFarlane, D. and Glover, K. (1988), “An  $h_\infty$  design procedure using robust stabilization of normalized coprime factors,” in *Decision and Control, 1988., Proceedings of the 27th IEEE Conference on*, pp. 1343–1348 vol.2.
- McFarlane, D. and Glover, K. (1992), “A loop-shaping design procedure using  $h_\infty$  synthesis,” *Automatic Control, IEEE Transactions on*, vol. 37, no. 6, pp. 759–769.
- Moore, J., Gangsaas, D., and Blight, J. (1981), “Performance and robustness trades in lqg regulator design,” in *Decision and Control including the Symposium on Adaptive Processes, 1981 20th IEEE Conference on*, pp. 1191–1200.
- Onodera, T., Masuda, Y., and Nakajima, A. (1981), “High-efficiency switching regulator using sub class e switching mode,” in *Telecommunications Energy Conference, 1981. INTELEC 1981. Third International*, pp. 132–137.
- Proakis, J.G. and Manolakis, D.K. (2007), *Digital signal processing principles, algorithms, and applications*, Prentice Hall.
- Redl, R., Sokal, N., and Balogh, L. (1990), “A novel soft-switching full-bridge dc/dc converter: Analysis, design considerations, and experimental results at 1.5 kw, 100 khz,” in *Power Electronics Specialists Conference, 1990. PESC '90 Record., 21st Annual IEEE*, pp. 162–172.
- Van der Schaft, A. (1992), “L2-gain analysis of nonlinear systems and nonlinear state-feedback  $h_\infty$  control,” *Automatic Control, IEEE Transactions on*, vol. 37, no. 6, pp. 770–784.

- Sepulchre, R., Janković, M., and Kokotović, P. (1997), *Constructive nonlinear control*, Springer.
- Shtessel, Y., Edwards, C., Fridman, L., and Levant, A. (2013), *Sliding mode control and observation*, Birkhäuser.
- Simon, D. (2006), *Optimal state estimation Kalman,  $H_\infty$ , and nonlinear approaches*, John Wiley & Sons Inc.
- Skogestad, S. and Postlethwaite, I. (2007), *Multivariable feedback control: analysis and design (2nd Edition)*, Wiley.
- Smedley, K.M. (1991), *Control art of switching converters*, Ph.D. thesis, California Institute of Technology.
- Sontag, E.D. (1998), *Mathematical control theory: deterministic finite dimensional systems, Second Edition*, Springer, New York.
- Åström, K.J. and Wittenmark, B. (2011), *Computer controlled systems theory and design*, Dover Publications Inc.
- Taylor, F. and Mellott, J. (1998), *Hands-on digital signal processing*, McGraw-Hill.
- Utkin, V. (1977), “Variable structure systems with sliding modes,” *Automatic Control, IEEE Transactions on*, vol. 22, no. 2, pp. 212–222.
- Vinnicombe, G. (2000), *Uncertainty and feedback,  $H_\infty$  loop-shaping and the  $v$ -gap metric*, World Scientific Publishing Company.
- Wester, G. and Middlebrook, R. (1973), “Low-frequency characterization of switched dc-dc converters,” *Aerospace and Electronic Systems, IEEE Transactions on*, vol. AES-9, no. 3, pp. 376–385.